CHAPTER III

THEORY

Molecular Sieves for Use in Catalysis

With the recent discoveries of molecular sieves materials containing other elements in addition to, or in lieu of, silicon and aluminum, the casual interchange of the terms "molecular sieve" and "zeolite" must be reconsiderd. In 1932 McBain proposed the term "molecular sieve" to describe a class of materials that exhibited selective adsorption properties. He proposed that for a material to be a molecular sieve, it must separate components of a mixture on the basis of molecular size and shape differences. Two classes of molecular sieves were known when McBain put forth his definition: the zeolites and certain microporous charcoals. The list now includes the silicates, the metallosilicates, metalloaluminates, the $AlPO_4$'s and silico- and metalloalumino-phosphates, as well as the zeolites. The different classes of molecular sieve materials are listed in Figure 3.1. All are molecular sieves, as their regular framework structures will separate components of a mixture on the basis of size and shape. The difference lies not within the structure of these materials, as many are structurally analogous, but in their elemental composition.

1. Molecular Sieves

A molecular sieve framework is based on an extensive three-dimensional network of oxygen ions containing generally tetrahedral type sites. In addition to the Si^{+4} and Al^{+3} that compositionally define the

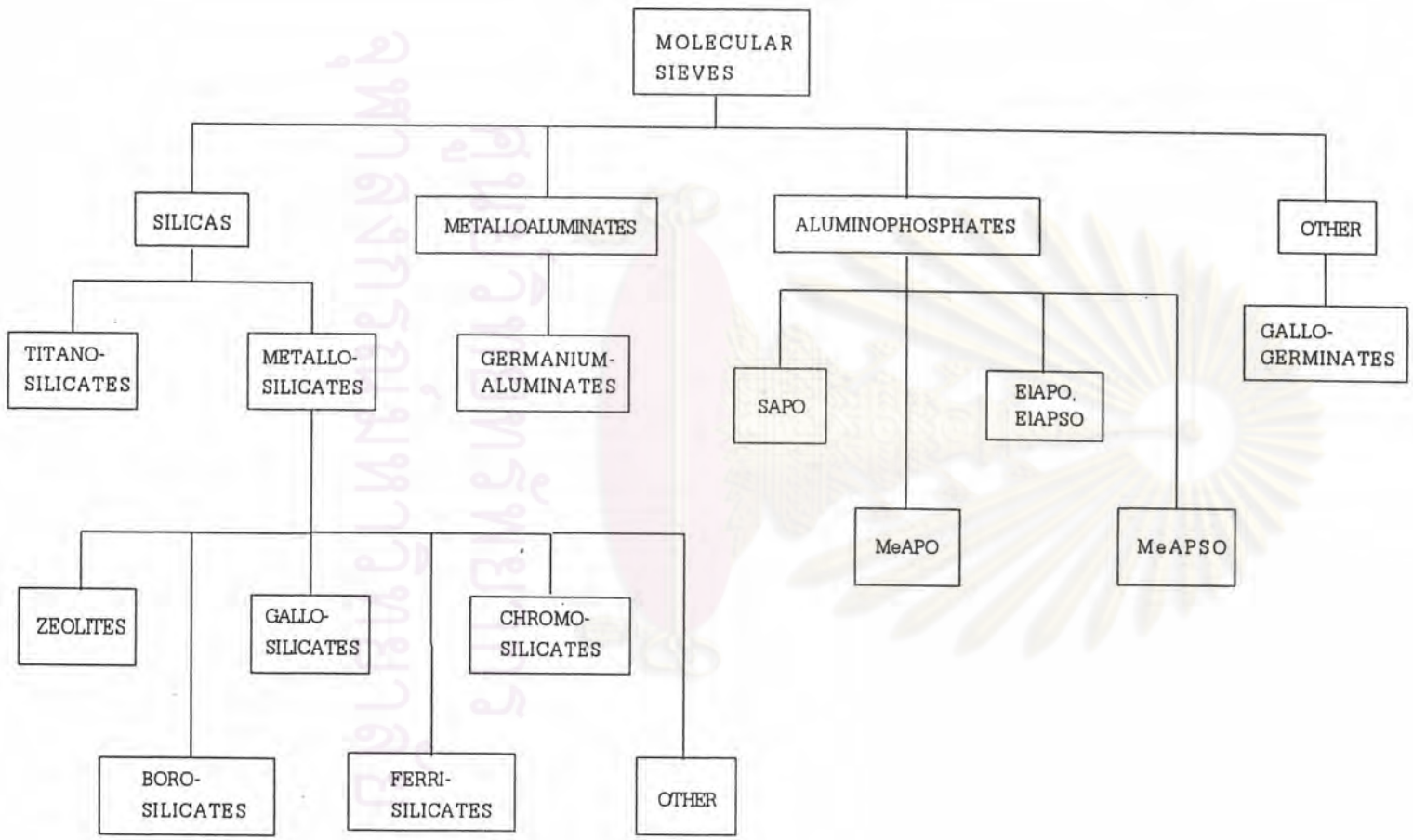

Figure 3.1 Classification of molecular sieve materials [51].

zeolite molecular sieves, other cations also can occupy these sites. These cations need not be isoelectronic with Si^{+4} or Al^{+3}, but must have the ability to occupy framework sites. The zeolite molecular sieves display a net negative framework charge; however, a molecular sieve framework need not display any charge. Molecular sieves containing only Si^{+4} in the tetrahedral sites will have a neutral framework and exhibit a high degree of hydrophobicity and no ion exchange capacity. The net charge on the $AlPO_4$ molecular sieves is also zero, arising from framework AlO_2^- and PO_2^+ units existion in equal amounts in these structures[51].

2. Zeolites

Zeolites are porous,crystalline aluminosilicates that develop uniform pore structure having minimum channel diameter of 0.3 to 1.0 nm. This size depends primarily upon the type of zeolite. Zeolites provide high activity and unusual selectivity in a variety of acid-catalyzed reactions. Most of the reactions are caused by the acidic nature of zeolites.

The structure of zeolites consists of a three-dimentional framework of SiO_4 or AlO_4 tetrahedra, each of which contains a silicon or aluminum atom in the center. The oxygen atoms are shared between adjoining tetrahedra, which can be present in various ratios and arranged in a variety of ways. The framework thus obtained contains pores, channels, and cages, or interconnected voids.

Zeolites may be represented by the general formular,

$$M_{x/n}[(AlO_2)_x(SiO_2)_y]wH_2O$$

where the term in brackets is the crystallographic unit cell. The metal cation of valence n is present to produce electrical neutrality since for each aluminum tetrahedron in the lattice there is an overall charge of -1 [52]. Misa proton, the zeolite becomes a strong Bronsted acid. As catalysts, zeolites are

unique in their ability to discriminate between reactant molecules and to control product selectivity, depending on molecular size and shape [53].

The catalytically most significant zeolites are those having pore openings characterized by 8-, 10-, and 12-rings of oxygen atoms. Some typical pore geometries are shown in Fig 3.2.

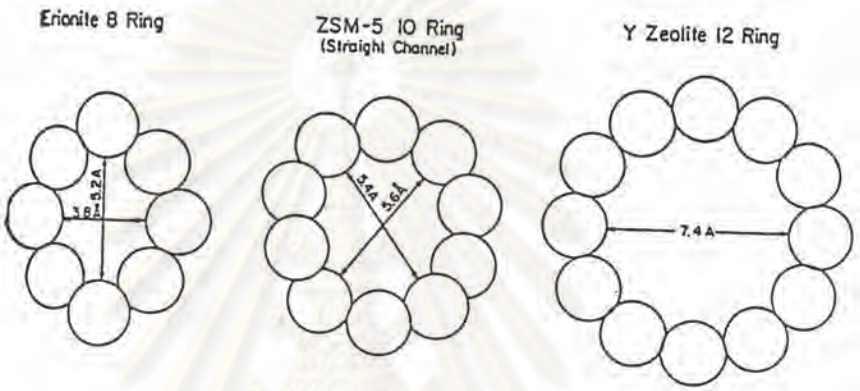

Figure 3.2 Typical zeolite pore geometries[54]

a) Small pore zeolites

Structures of some of these small pore zeolites are illustrated in Fig.3.3.

The erionite structure, Fig.3.3.(a), is hexagonal, containing "supercage" supported by columns of cancrinite units linked through double-6-rings (D6R). Access to, and between, the supercages is gained through 8-rings.

In the chabazite framework, Fig. 3.3.(b), the D6R layer sequence is ABCABC, and the D6R units are linked together through tilted 4-rings. The framework contains large ellipsoidal cavities, Fig. 3.3.(c), each entered through six 8-rings. These cavities are joined together via their 8-rings, forming a 3-dimensional channel system.

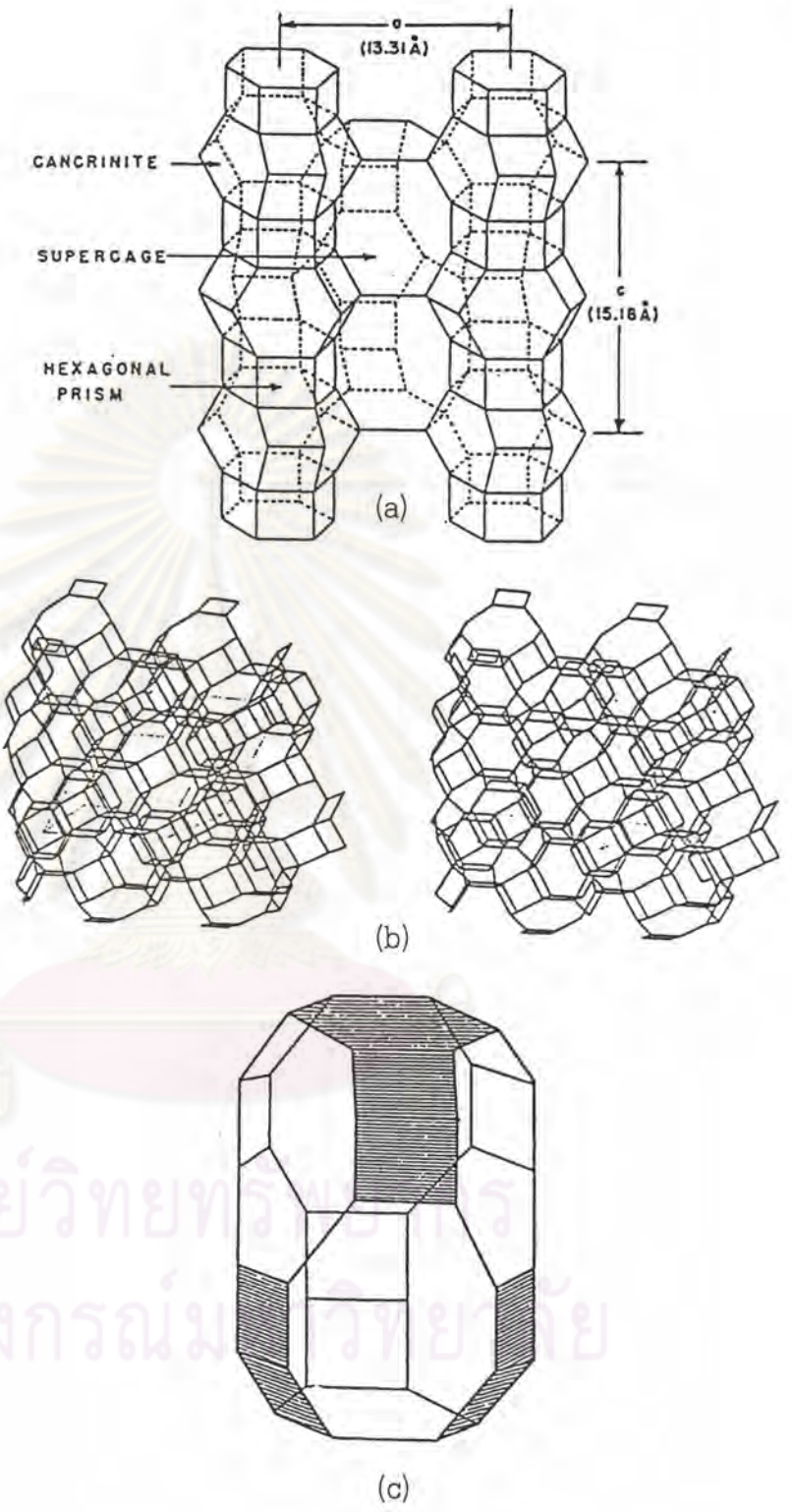

Fig. 3.3 Small pore zeolites (a) Erionite framework (b) Chabazite framework (c) Chabazite cavity[54].

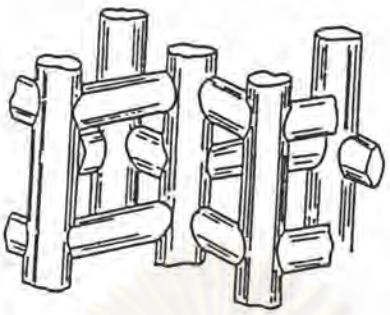

Fig. 3.4 ZSM-5 channel system[54].

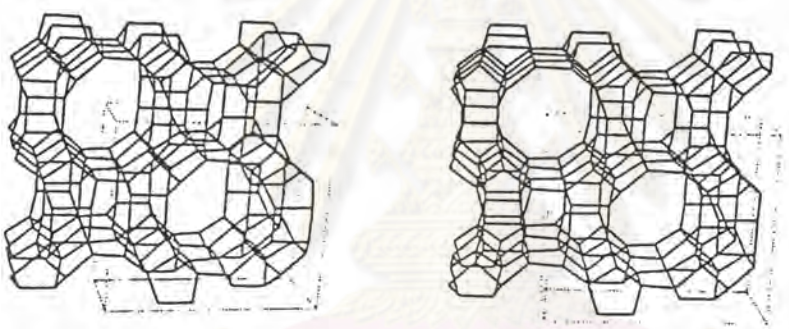

(a)

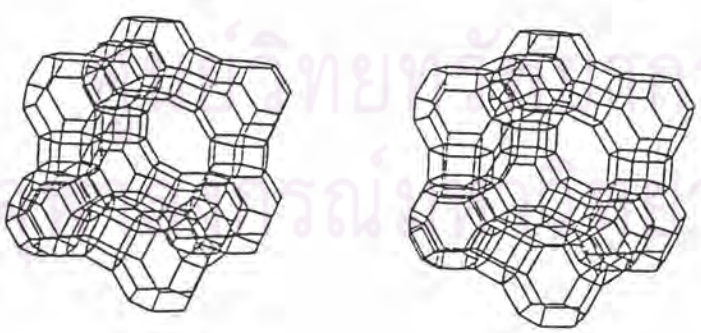

(b)

Fig 3.5 Large pore zeolites (a) Mordenite framework (b) Faujasite framework[54].

b) Medium pore zeolites

Zeolites ZSM-5 has orthorombic symmetry Pnma with cell parameters a = 20.07, b = 19.92, c = 13.42 A°. The channel system, represented in Fig. 3.4, consists of straight channels running pararell to [010] and intersecting sinusoidal channels parallels to [100]. The channels are ellipsoidal with 10-ring openings, having the approximate free dimensions 5.4x5.6 A° (straight channels) and 5.1x5.4 A° (sinusoidal channels) based on oxygen radii 1.35 A° . Fig.3.4.2 shows a stereo-pair drawing of the ZSM-5 framework viewed along [010].

c) Large pore zeolites

The faujasite structure, Fig. 3.5.(a), is built up of truncated octahedra interconnected via D6R units. Faujasites contain extremely large supercages (~ 13 A° diameter) entered into through 12-rings.

Mordenite, Fig.3.5.(b), is characterized by a one-dimensional system of parallels elliptical channels, defined by 12-rings.

3. $AlPO_4$ Molecular Sieves

The aluminophosphate family of molecular sieves are microporous crystalline oxides, many of which, like the zeolites, contain pores within their framework structure that are molecular in dimension. In the aluminophosphates ($AlPO_4$'s) the framework sites are occupied by Al^{3+} or P^{+5}. The average of the ionic radii of Al^{3+} (0.39 A°) and P^{+5} (0.17 A°) is 0.28 A°, which is similar to the ionic radius of Si^{+4} (0.26 A°). The notable feature of the $AlPO_4$ composition is the invariant Al_2O_3/P_2O_5 ratio , which is indirect contrast with the variable compositions of silica/alumina found in the zeolite structures. Unlike the zeolite molecular sieves, which contain Al^{3+} and Si^{+4} in tetrahedral positions and exhibit a net negative framework charge, the $AlPO_4$ materials may contain aluminum in coordination other than tetrahedral, and a

framework that is neutral. Structural diversity is found in the $AlPO_4$ materials, even with such limited variation in chemical composition. The overall composition of the $AlPO_4$ molecular sieves is written as :

$$xR \quad Al_2O_3 \quad 1.0(+/-0.2)P_2O_5 \quad yH_2O$$

where R is an organic amine or quarternary ammonium ion. The quantities *x* and *y* represent the amount of organic or water that fills the pores of the crystal, as the $AlPO_4$ require counter-ions [51].

4. SAPO Molecular Sieves

Attempts were made to incorporate phosphorus into other zeolites structures during synthesis with moderate success. Phosphorus-containing zeolites were prepared from alumino- silicate gel systems. In most of the zeolite systems it appears that (Al+P) substitutes for 2Si, though in some cases excess P is observed and proposed to substitution for silicon. Such substitution would still result in a net negative framework charge.

In addition to the incorporation of phosphorus into zeolite gels to produce silicoaluminophosphate materials, silica can be considered to incorporate into the $AlPO_4$ structure to form such SAPO materials. The synthesis of a large number of SAPO molecular sieves under the conditions used for preparation of the $AlPO_4$ materials appears to be fruitful in generating both zeolite-like and $AlPO_4$-like structures, as well as structures that are not found in either system. Three novel structures have been prepared in the SAPO system that have no structural counterpart in the other molecular sieve compositions. A list of the SAPO molecular sieves prepared is given in Table 3.1. The list analogous structure, if known, and the ring size, as well as the oxygen and water adsorption capacities.

Table 3.1 SAPO molecular sieves synthesized, their structure type, ring size, and selected adsorption capacities.

NAME	STRUCTURE TYPE	RING SIZE	ADSORPTION CAPACITIES [a]	
			O_2	H_2O
SAPO-5	$AlPO_4$-5	12	0.23	0.31
SAPO-11	$AlPO_4$-11	10	0.13	0.18
SAPO-16	$AlPO_4$-16	6	[b]	[b]
SAPO-17	Erionite	8	0.2	0.35
SAPO-20	Sodalite	6	0	0.40
SAPO-31	$AlPO_4$-31	10	0.13	0.21
SAPO-34	Chabazite	8	0.32	0.42
SAPO-35	Levynite	8	0.26	0.48
SAPO-37	Faujasite	12	0.37	0.35
SAPO-40	Novel	12	0.31	0.33
SAPO-41	Novel	10	0.10	0.22
SAPO-42	Zeolite A	8	[b]	[b]
SAPO-44	Novel	8	0.28	0.34

[a] Determined by standard McBain-Bakr gravimetric techniques after calcination (500-600 °C in air) to remove the organic. O_2 measured near saturation at -183 °C, H_2O at ambient temperature.

[b] Sufficient adsorption data are not available for SAPO-16 and -42.

Synthesis of SAPO molecular sieves

The synthesis of the $AlPO_4$ molecular sieves, though similar in some ways to that of the zeolite materials, does have some notable differences. Like the zeolites, the $AlPO_4$ materials are synthesized hydrothermally with a preferred temperature range between 125 and 200 °C. Unlike the zeolite molecular sieves, however, the presence of organic additives appears necessary to promote crystallization in the aluminophosphate system.

The synthesis method used in the preparation of SAPO molecular sieves is equivalent to that of the $AlPO_4$ molecular sieves. The preferred source of aluminum is boehmite, a reactive hydrated alumina, phosphorus is added as phosphoric acid. The source of silica used in the synthesis is silica sol. The compositional range of the silicoaluminophosphates is of :

$$0\text{-}0.3R \quad (Si_xAl_yP_z)O_2$$

where, in the anhydrous form,x,y,and z are the mole fractions of silicon aluminum and phosphorus in the range of 0.01 to 0.98, 0.01 to 0.60, and 0.01 to 0.52, respectively ($x + y + z = 1$). As in the synthesis of the zeolites and the aluminophosphates, the organic amine or ammonium cation aids in directing the structure type produced. However, the presence of the silicon in the reaction mixture also contributes to directing the structure. The most notable result of the role of the silicate in the reaction mixture is the production of novel SAPO structures. Tetraethylammonium ion is a template for $AlPO_4$-5 and $AlPO_4$-18 in the aluminophosphate system, but addition of silicate to the $AlPO_4$ gel using this organic amine results in the formation of SAPO-34, which is a chabazite-type structure. Structures with no $AlPO_4$ or zeolite equivalent include SAPO-40, and -44 prepared from reaction mixtures containing TPA, TBA, and cyclohexylamine, respectively.

A fundamental question that arises regarding the substitution of silicon into the $AlPO_4$ structural framework is the location of this substituted ion. As Figure 3.6, from a structural standpoint we can consider them. In the $AlPO_4$ framework, silicon theoretically can substitute for aluminum, phosphorus, or both.

If the silicon substitutes for aluminum, the charge on the framework will be positive, giving rise to anionic exchange properties; substitution for phosphorus will result in an anionic framework similar to the

zeolite molecular sieve; no net change in framework will be observed if both aluminum and phosphorus are simultaneously substituted with two silicon atoms. The ability to exchange cations as well as observed acid activity in the SAPO materials indicates that the silicon does, indeed, substitute for phosphorus although the substitution of both aluminum and phosphorus is also indicated for several structures. SAPO-34 and SAPO-37 both have mole

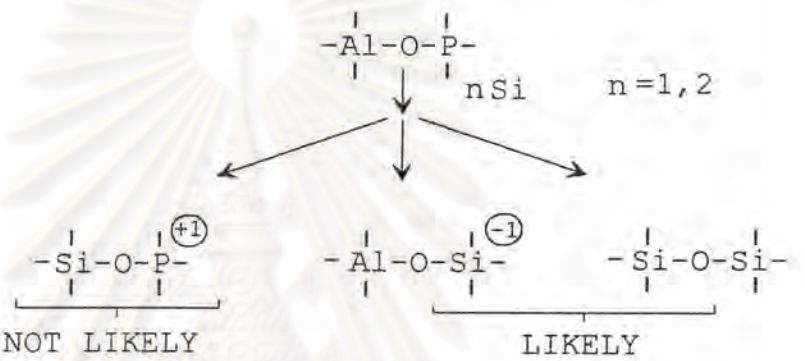

Figure 3.6 Effect of silicon incorporation on framework charge of SAPO molecular sieves[51].

fractions for $Si_xAl_yP_z$ with $x+z = y$, indicative of substitution of silicon for phosphorus. For SAPO-5, and SAPO-11, $x+z$ is greater than y, which is evidence for substitution of two silicon atoms for (Al + P) in addition to substitution of Si for P [51].

The substitution of silicon may be via the second and third mechanisms. Thus, these materials have anionic frameworks like zeolites and should have Bronsted acid sites[55].

Acidity

Classical Bronsted and Lewis acid models of acidity have been used to classify the active sites on zeolites. Bronsted acidity is proton donor acidity; a

trigonally coordinated alumina atom is an electron deficient and can accept an electron pair, therefore behaves as a Lewis acid [53,56].

Recently it has been reported the mean charge on the proton was shifted regularly towards higher values as the Al content decreased [53]. Simultaneously the total number of acidic hydroxyls, governed by the Al atoms, were decreased. This evidence emphasized that the entire acid strength distribution (weak, medium, strong) was shifted towards stronger values. That is, weaker acid sites become stronger with the decrease in Al content.

An improvement in thermal or hydrothermal stability has been ascribed to the lower density of hydroxyls groups which parallel to that of Al content [52]. A longer distance between hydroxyl groups decreases the probability of dehydroxylation that generates defects on structure of zeolites.

Generation of Acid Centers

Protonic acid centers of zeolite are generated in various ways. The Bronsted acidity due to water ionization on polyvalent cations described below.

$$M^{n+} + xH_2O \text{ -----> } M(OH)_x^{(n-x)+} + xH^+ \qquad (3.1)$$

The exchange of monovalent ions by polyvalent cations could improve the catalytic property. Those highly charged cations create very acidic centers by hydrolysis phenomena.

Bronsted acid sites are also generated by the reduction of transition metal cations. The concentration of OH groups of zeolite containing transition metals was noted to increase by reduction with hydrogen at 250-450 °C at to increase with the rise of the reduction temperature [51].

$$Cu^{2+} + H_2 \text{ -----> } Cu^{\circ} + 2H^{+} \quad (3.2)$$

$$Ag^{+} + 1/2\ H_2 \text{ -----> } Ag^{\circ} + H^{+} \quad (3.3)$$

The formation of Lewis acidity from Bronsted sites would be reversible reaction of water ionization. The dehydration reaction decreases the number of protons and increases that of Lewis sites.

Bronsted (OH) and Lewis (-Al-) sites can be present simultaneously in the structure of zeolite at high temperature. Dehydroxylation is thought to occur in ZSM-5 zeolite above 500 °C and calcination at 800 to 900 °C produces irreversible dehydroxylation which causes defection in crystal structure of zeolite.

The enhancement of the acid strength of OH groups is recently proposed to be pertinent to their interaction with those aluminum species sites. Partial dealumination might, therefore, yield a catalyst of higher activity while severe steaming reduces the catalytic activity.

Shape Selectivity

Many reactions involving carbonium ions intermediates are catalyzed by acidic zeolites. With respect to a chemical standpoint the reaction mechanisms are not fundamentally different with zeolites or with any other acidic oxides. What zeolite add is shape selectivity effect. The shape selective characteristics of zeolites influence their catalytic phenomena by three modes; reactants shape selectivity, products shape selectivity and transition states shape selectivity [52,57-58]. These type of selectivity are depicted in Figure 3.7.

Reactant or charge selectivity results from the limited diffusibility of some of reactants, which cannot effectively enter and diffuse inside crystal pore structures of the zeolites.

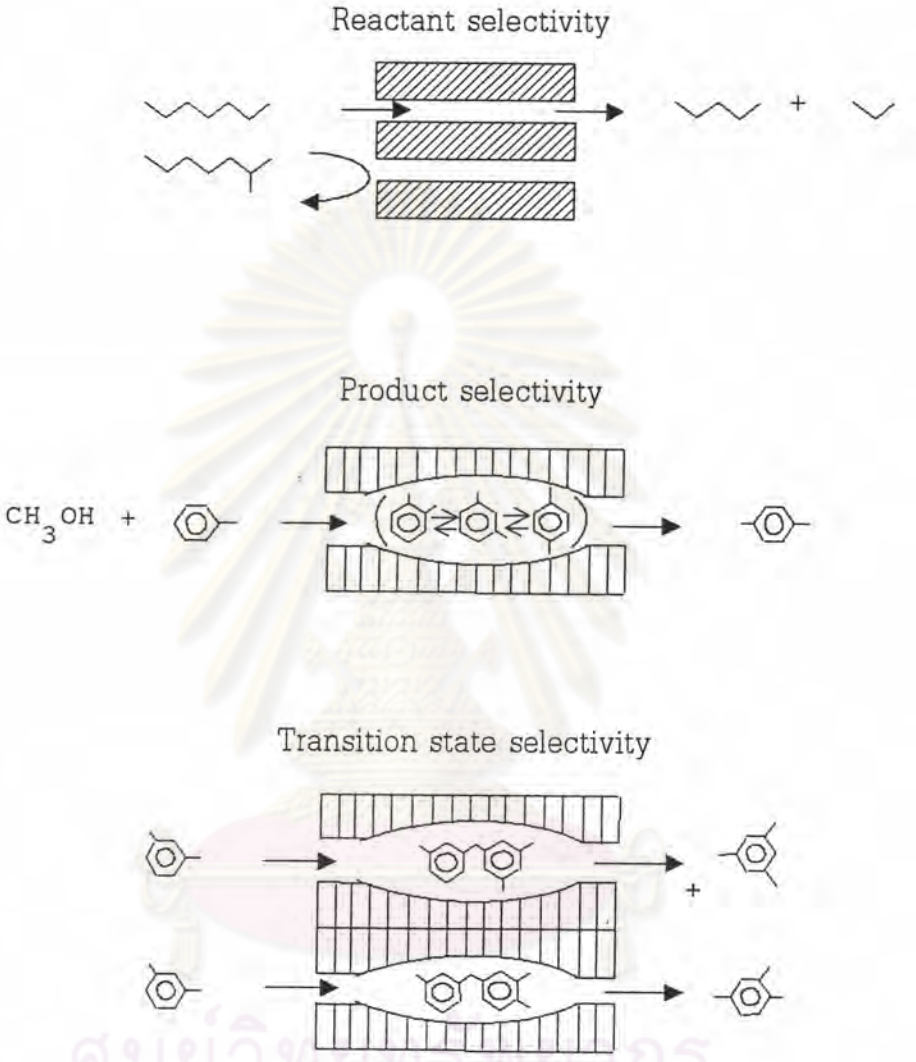

Figure 3.7 Diagram depicting the three types of selectivity : reactant, product,and transition-state type selectivity[52].

Product shape selectivity occurs as slowly diffusing product molecules cannot escape from the crystal and undergo secondary reactions.

Restricted transition state shape selectivity is a kinetic effect arising from local environment around the active site, the rate constant for a certain reaction mechanism is reduced if the space required for formation of necessary transition state is restricted.

The critical diameter (as opposed to the length) of the molecules and the pore channel diameter of zeolites are important in predicting shape selective effects. However, molecules are deformable and can pass through openings which are smaller than their critical diameters. Hence, not only size but also the dynamics and structure of the molecules must be taken into account.

Reaction Mechanism of Methanol to Olefins

The reaction of methanol to hydrocarbon products is vigously exothermic, with a theoretical adiabatic temperature rise of about 600 °C. The reaction path is believed to pass through a number of series and parallel steps. The mechanism is complex and is discussed elsewhere . A simplified path is given below[54,59].

$$2\ CH_3OH \ <===>\ CH_3OCH_3 + H_2O \qquad (3.4)$$

$$CH_3OCH_3 \ ====>\ \text{Light Olefins} + H_2O \qquad (3.5)$$

$$\text{Light Olefins} + CH_3OCH_3 \ ====>\ \text{Heavy Olefins} + H_2O \qquad (3.6)$$

$$\text{Heavy Olefins} \ ====>\ \text{Aromatics} + \text{Paraffins} \qquad (3.7)$$

$$\text{Aromatics} + CH_3OCH_3 \ ====>\ \text{Higher aromatics} + H_2O \qquad (3.8)$$

The first step in the reaction sequence is the dehydration of methanol to an equilibrium mixture of dimethylether (DME), methanol and water. The DME then reacts further to form a mixture of light olefins. As the concentration of DME is depleted, the equilibrium of reaction 3.4 is disturbed and further dehydration of methanol takes place. The DME alkylates the light olefins (mostly propylene and butenes) to higher olefins, which can then further react with one another to form aromatics and paraffins. If any residual DME remains at the point where aromatics form, those aromatics are readily alkylated to higher carbon number of C_{10}. The heaviest component is durene (1,2,4,5-tetramethylbenzene), which lies near the high end of the gasoline boiling range. No components with normal boiling points above the gasoline boiling range are produced[60].

The early work of Chang [54] showed that high temperature favours selectivity to light olefins. Mobil found that by combining the factors of reduced catalyst activity with high operating temperatures, it was possible to switch the Methanol To Gasoline (MTG) selectivity towards an olefin rich spectrum. This route was named the Methanol To Olefins (MTO) process, and gives a product that is rich in propylene and butenes together with a good aromatic rich C_5+ gasoline fraction.

Voltz and Wise [61] has proposed scheme A to contain a direct path to olefins from methanol:

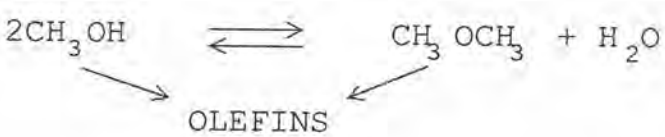

Scheme A

The reaction path formation may be viewed essentially as composed of three key steps - ether formation, initial C-C bond formation, and aromatization

with H-transfer. The final stages, comprising olefins condensation, cyclization and H-transfer over acidic catalysts, have been well studied and proceed via classical carbenium mechanisms [62-64].

The mechanism of polymethylbenzenes formation will, however, be discussed since these compounds are peculiar to the methanol transformation reaction.

1. Ether formation

The mechanism of ether formation from alcohols over oxide catalysts, particularly Al_2O_3, has been extensively investigated. The bulk of work has concentrated on alcohols having β-hydrogens. Several comprehensive surveys have been published [65-68].

In contrast, the literature on methanol dehydration is relatively sparse. Methanol etherification is similar in many respects to that of the higher alcohols; however, since methanol lacks a parent olefin, sufficient differences may be found as to warrant its discussion here.

The dehydration of methanol on alumina and amorphous silica-alumina monitors the effect of a series of nitrogenous poisons (various amines and N-heterocycles) or dimethylether formation. Silica-alumina is irreversibly poisoned, while alumina is reversibly poisoned. This is taken as evidence that there action over alumina involved surface methoxy groups:

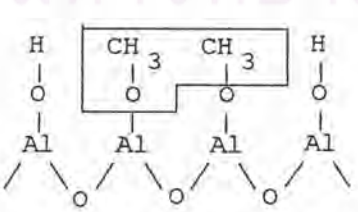

This interpretation is based on the assumption that bases such as diethalamine dissociatively but reversibly chemisorb on alumina.

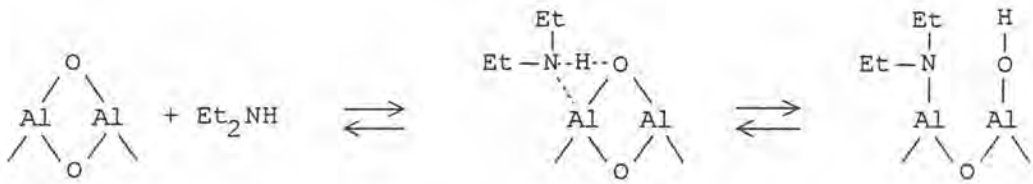

Because of the greater nucleophilicity of N vs O, the nitrogenous base competes with methanol for the surface oxygen, thereby inhibiting methoxylation. On the otherhand, the reaction over silica-alumina involves Bronsted sites, which are strongly poisoned by nitrogen base, forming stable quaternary ions. According to these investigators ether formation over silica- alumina may be represented by the following scheme:

$$CH_3OH + H^+ \text{-----> } CH_3OH_2^+$$

$$CH_3OH_2^+ + CH_3OH \text{-----> } (CH_3)_2O + H_2O + H^+$$

The kinetics of methanol dehydration over silica-alumina at 160-200 °C and the rate expression can derive as follow:

$$V = ka\sqrt{P_a}\,/(1 + a\sqrt{P_a}$$

where P_a is the alcohol partial pressure. It was concluded that the rate-limiting step cannot be the interaction of two surface alcoholate groups, which would lead to a rate equation of the form

$$r = k\theta^2 = kaP/(1 + aP)^2$$

At low pressures the reaction order would be unity, which is not in agreement with the observed half-order. Figueras et al. proposed two modes of

chemisorption, both of which assumed the concerted action of acidic and basic centers. Nucleophilic attack on carbon by the basic site would generate CH_3^+, which then interacts with an acid-generated surface methoxy group to give ether. The observed half-order was rationalized on the ground that one of the species, CH_3O or CH_3, must be reversibly adsorbed. Primary carbonium ions are much less stable than alkoxide structures, and therefore equilibrium with the undissociated species would be readily established:

The thermal decomposition of methanol adsorbed on alumina was investigated by using deuterium labeling. Desorption of methanol started at 77°C. At T >77°C,significant concentrations of CH_2O, H_2O, and CH_3OCH_3 were observed, and above 427 °C, CO was predominant while CH_4 was significant. Coadsorption of CD_3OD and CH_3OH was carried out. Under desorption at T<237 °C, the ether contained only CH_3OCH_3, CH_3OCD_3, and CD_3OCD_3, while at higher temperatures deuterium distribution became random. Thermal decomposition of CH_3OH_{ad} in the presence of gaseous CD_3OCD_3 gave only CH_3OCH_3, indicating that ether is formed by a bimolecular reaction between adjacent surface methoxides.

Schmitz [68] studied the dehydration of methanol over silica-alumina at 289-418 °C and found that the reaction becomes first-order in methanol at the higher temperatures. Interestingly, Schmitz observed an induction period, possibly the result of the initial formation of surface carboxylate groups, which, though not ether intermediates, could nevertheless

influence the initial rate of dehydration by occupying active sites. Another explanation might involve competitive sorption of product water prior to establishment of steady-state with respect to surface hydroxyl concentration.

Detrekoy and Kallo [69] investigated the dehydration of methanol over clinoptilolite by infrared spectroscopy. Methanol (6 torr) was adsorbed on H-clinoptilolite at various temperatures. At 25 °C the 3620 cm^{-1} band (acidic OH on clinoptilolite) disappears and two bands at 2950 and 2840 cm^{-1} (CH stretching) appear. Upon evacuation, the CH bands decreased significantly; however, the OH band did not reappear. This indicated that only weakly adsorbed methanol is removed. Absorption at 160°C followed by evacuation caused only a partial disappearance of the 3620 cm^{-1} band and a lower intensity of the 2950 and 2840 cm^{-1} bands. At 400°C, methanol can be completely removed and the CH bands are shifted to 2860 and 2960 cm^{-1}, indicating the presence of surface methoxyls.

Detrekoy and Kallo found that methanol dehydration also occurs on dehydroxylated (at T > 400°C) clinoptilolite. They attribute this to the formation of Bronsted sites from Lewis sites by hydration during reaction with methanol. The following mechanism was proposed:

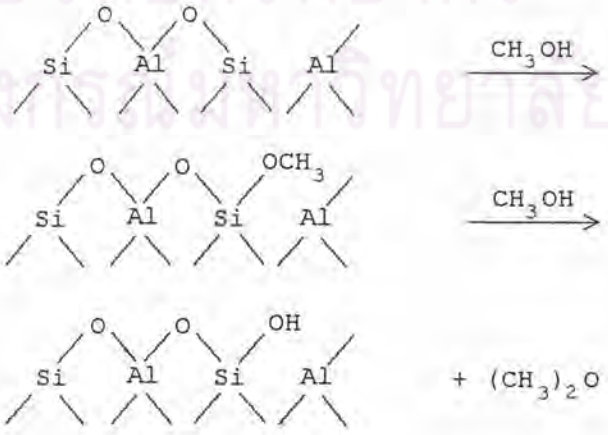

Further reaction would be catalyzed by the acidic OH groups thus generated.

In a study of methanol reaction on synthetic germanic near-faujasite using ^{13}C-NMR, Derouane et.al. [70] observed partial methoxylation of the surface at 300 °C, with ether formation. Surface methoxyls could be hydrolyzed with water back to methanol at 25°C. Additional small amounts of dimethyl ether and surface formate were also found after hydrolysis.

In summary, the weight of evidence favors the intermediacy of surface alkoxyls in ether formation from alcohols. Beranek and Kraus [71] conclude that the mechanism involves essentially a nucleophilic substitution whereby the surface alkoxide is attacked by another molecule, either from the gas phase or from a weakly adsorbed state. Arguments in support of this mechanism were summarized as follows:

1. "Similar products are obtained by the decomposition of metal alkoxides containing nog-hydrogens and by the reaction of corresponding alcohols on alumina at liwer temperatures".
2. "Acetic acid and pyridine are poisons for the formation of ethers".
3. "The different degrees of water inhibition on the ether and olefin formation from ethanol on alumina, and the agreement of ether/ethylene selectivity ratios found experimentally with those calculated by the Monte Carlo simulation of the hydrated surface of alumina".
4. "Correlation between the rate of ether formation from methanol and the surface concentration of ethoxide species determined by IR spectroscopy".
5. "The positive value of the Taft reaction parameter for the formation of ether incontrast to negative values for the olefin formation on the same catalyst".

The second part of Statement 5 applies only to C_2^+ alcohols.

2. Hydrocarbon Formation

The mechanism of initial C-C bond formation from methanol is an unresolved question at present. Hypothetical mechanisms abound in the literature,and run the gamut from carbene to free radical schemes. As of this writing, however, little supporting experimental evidence has appeared. It seems appropriate, mevertheless, to survey and discuss the diverse entries in this "mechanism sweepstakes."

2.1. Via Surface Alkoxyls

Among contemporary investigators, the first to consider this question were Topchieva and collaborators in connection with a study of the adsorption of methanol vapor on SiO_2, SiO_2-Al_2O_3 and Al_2O_3 surfaces. It was found that a portion of the methanol was irreversibly adsorbed on SiO_2-Al_2O_3 and Al_2O_3, which upon heating and pumping to 400 °C evolves C_2H_4, C_2H_6, CO, and CO_2. The formation of surface methoxy groups was regarded as the primary step. Hydrocarbon formation was consideredtooccur by condensation of methoxy groups, accompanied by dehydration and H-transfer.The mechanistic details of this condensation were not specified. Subsequently, Heiba and Landis [72] showed that the thermolysis products of aluminum alkoxides are virtually identical to the products of alumina-catalyzed decomposition of alcohols or ethers, as shown in Table 3.2. It is seen that the main products are CH_4, H_2, CO, $(CH_3)_2O$, and smaller amounts of C_2H_4 and C_3H_6. Based on the observation that $Al(OCH_2\Phi)_3$ decomposed more readily than $Al(OCH_3)_3$, it was concluded that cleavage of the C-O bond is a heterolytic process, with the flow of electrons in the direction of Al, leaving a positively charged carbon moiety as the reactive intermediate. A negative activation entropy was observed, suggesting a cyclic transition state. A free radical

mechanism was rejected on the basis of negligible reactivity over nonacidic solids, e.g., quartz, at temperatures up to 450°C.

Table 3.2 Decomposition of Methyl Derivatives [72].

Product	$Al(OCH_3)_3$ at 385 °C (mol%)	CH_3OH over Al_2O_3 at 450 °C 0.5 LHSV	$(CH_3)_2O$ over Al_2O_3 at 450 °C 0.5 LHSV
CH_4	22.5	Major	Major
H_2	35.2	Major	Major
CO	31.1	Major	Major
C_2H_4	1.3	Minor	Minor
C_3H_6	2.5	Minor	Minor
$(CH_2)_2O$	7.1	Major	Major
Other	0.3	Minor	Minor

In a later study the thermal decomposition of methoxides of Na, Mg, and Al and the compound $Na[Al(OMe)_4]$ was reported by Pfeifer and Flora [73]. Ethene was the only hydrocarbon product observed.

2.2. Carbenes and Carbenoids

Venuto and Landis proposed an α-elimination mechanism to account for olefins formed during methanol dehydration to dimethyl ether over NaX at 260°C, as reported by Mattox [74], and from methanol reaction over ReX and ZnX at 330-390 °C, as observed by Schwartz and Ciric [75]. According to this view, methanol adsorbed on the zeolite surface loses water to form a divalent carbenoid species, which then polymerize to form olefins:

$$H\text{-}CH_2\text{-}OH \longrightarrow H_2O + :CH_2$$

$$n{:}CH_2 \longrightarrow (CH_2)n, \quad n = 2, 3, 4, 5$$

Swabb and Gates studied the dehydration of methanol over H-mordenite at 155-240°C. Traces of olefin were detected at 240°C. It was speculated that the olefins were formed by an α-elimination mechanism. where bond scission is facilitated by cooperative action of acidic and basic sites in the zeolite lattice:

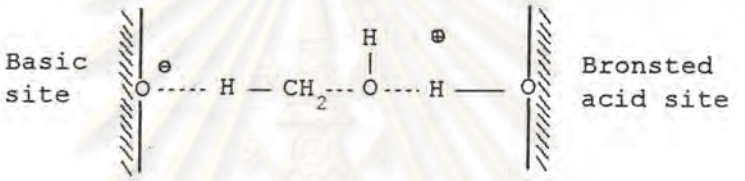

Salvador and Kladnig [76] investigated the surface reactions of methanol on HY and NaY at 20-350 °C using IR, GLC, adsorption isotherm, and TGA techniques. At room temperature, physical adsorption occurs on both zeolites. With HY, methoxylation of surface hydroxyl groups begins at 20 °C, reaching a maximum at 130 °C. At 120 °C, dimethyl ether formation begins and reaches a maximum at 210 °C, and around 250 °C secondary cracking reactions occur forming predominantly butane and propene. This was accompanied by darkening of the catalyst due to coking which was enhanced with a further temperature increase. Salvador and Kladnig favored an α-elimination mechanism to explain olefin formation. They differed with the acid-base mechanism of Swabb and Gates, proposing that the generation of carbenoid species occurs by decomposition of the methoxylated surface:

$$\geq SiOCH_3 \longrightarrow \geq SiOH + :CH_2$$

Condensation of the carbene would give olefin. Alkanes were assumed to arise via H-transfer reactions.

An α-elimination mechanism involving a carbenoid intermediate was also proposed by Chang and Silvestri for methanol reaction over ZSM-5. However, it was considered unlikely the olefins were formed by polymerization of the diradical intermediate. On view of the high reactivity of carbenes, the probability of such an event would be low, as demonstrated in studies on ketene photolysis. By the same token, the presence of free carbenes would be unlikely. Rather, a concerted reaction between methylene donor and acceptor was proposed involving simultaneous α-elimination and sp^3 insertion into methanol or dimethyl ether as the primary step.

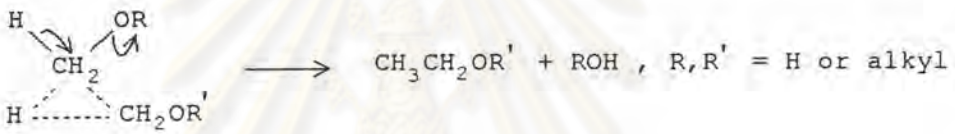

An ionic mechanism involving methyl cations was rejected since these species would be expected to form methane readily via hydride abstraction from methanol, dimethyl ether, or hydrocarbons. The reaction

$$CH_3^+ + CH_3OH \text{ -----> } C^+H_2OH + CH_4$$

is extremely rapid in the gas phase. However, methane normally accounts for $\leq$ 1% of the hydrocarbons formed over ZSM-5. Note also that C^+H_2OH could deprotonate to formaldehyde which is not observed over ZSM-5.

The presence of small amounts of methyl ethyl ether in the products of methanol conversion over ZSM-5 was reported by Chang and Silvestri . Cormerais et al. found MeOEt among the products of dimethyl ether decomposition over silica-alumina at 423 K. This compound could either be a key reaction intermediate or simply a secondary product of the methanol-to-ethene reaction. From kinetic evidence, Cormerais et al. deduced

that this compound was not formed via reaction of Me_2O with ethene. It was determined that in the presence of excess ethene, amounting to 30X that of the products from Me_2O, the rate of MeOEt formation from Me_2O was increased by only a factor of 5. More significantly, the formation of propene from MeOEt was more than 10 times faster than from Me_2O. In view of the observed unreactivity of ethene, it was concluded that propene is formed by two successive CH_2 insertions into Me_2O, leading to MeOPr, which cleaves to propene. Another set of experiments gave analogous results for C_4 hydrocarbons.

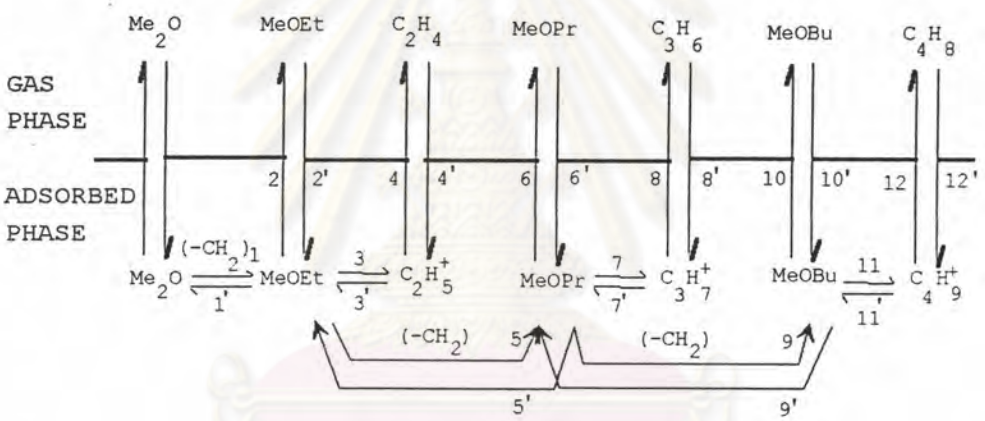

Figure 3.8 "Rake" mechanism for dimethyl ether conversion to hydrocarbons [77].

Cormerais et al. [77,78] proposed a chain growth "rake mechanism," Figure 3.8, to explain their results. In this scheme, chain growth occurs by carbene insertion into surface alkoxy species, which are transformed into olefins via carbenium ions.

2.3. Oxonium Ions and Yields

In their mechanism Chang and Silvestri left open the question of stabilization of the intermediate carbene in the transition state. A plausible resolution of this question may be found in the mechanism of van den Berg et al. [79]. In their view, dimethyl ether from methanol dehydration reacts with a Bronsted acid site to form a dimethyloxonium ion I, which reacts with another molecule of dimethyl ether to form, via II, and after elimination of methanol, a trimethyloxonium ion III:

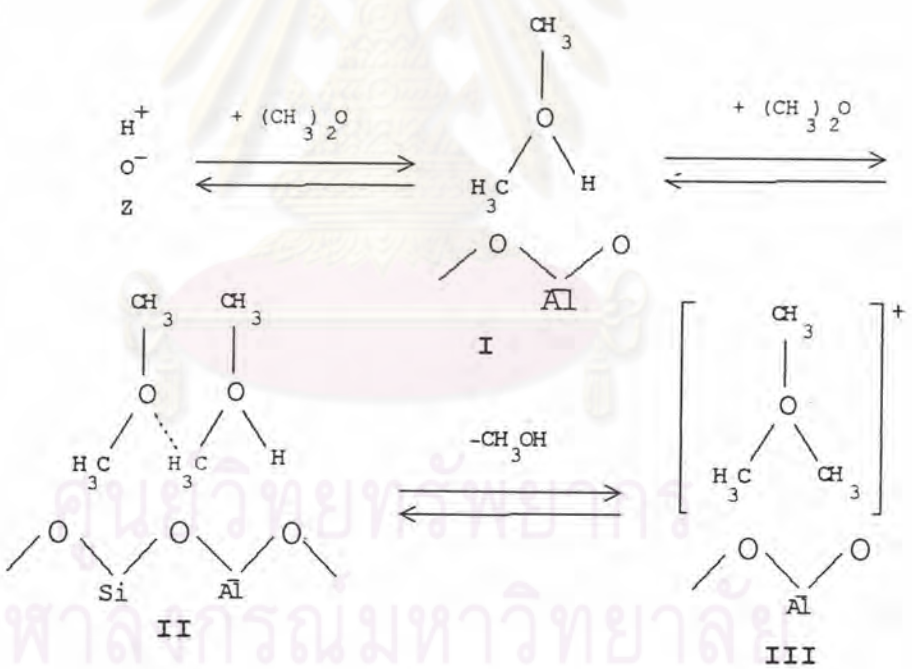

the critical step in their proposal is a Stevens-type intramolecular rearrangement of the trimethyloxoniom ion III to a methylethyloxonium ion V:

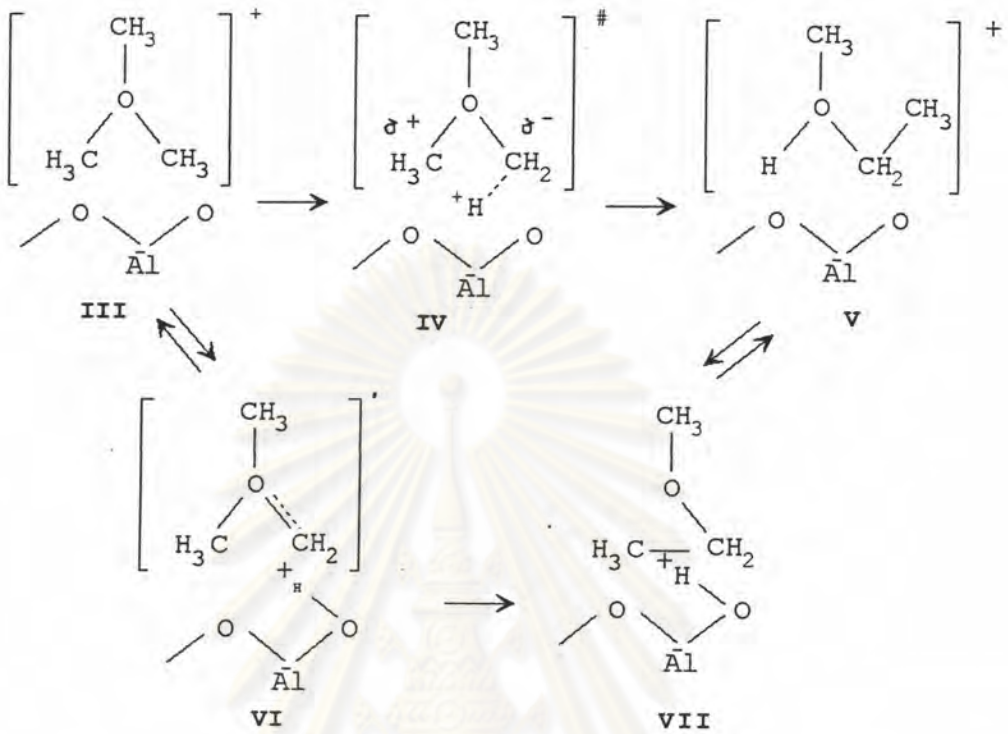

Structure VI, which is equivalent to the oxonium ylid $(CH_3)_2O^+CH_2^-$, is seen to contain the stabilized C_1 carbenoid species. Cis-insertion of the carbenoid into the adjacent C-O leads to C-C bond formation. The formation of ylid depends on the assumption that the conjugate basic sites in ZSM-5 are sufficiently strong to induce polarization of a C-H bond on a methyl group. As indicated previously, the ab initio field calculations of Beran and Jiru [80] lend support to this assumption.

An alternate cationic mechanism involving carboxonium ions was considered by van den Berg [81]. In this variation the carboxonium ion is generated by hydride abstraction. Van den Berg presented the following scheme comparing the steps in the alkoxonium Route (A) and the carboxonium Route (B).

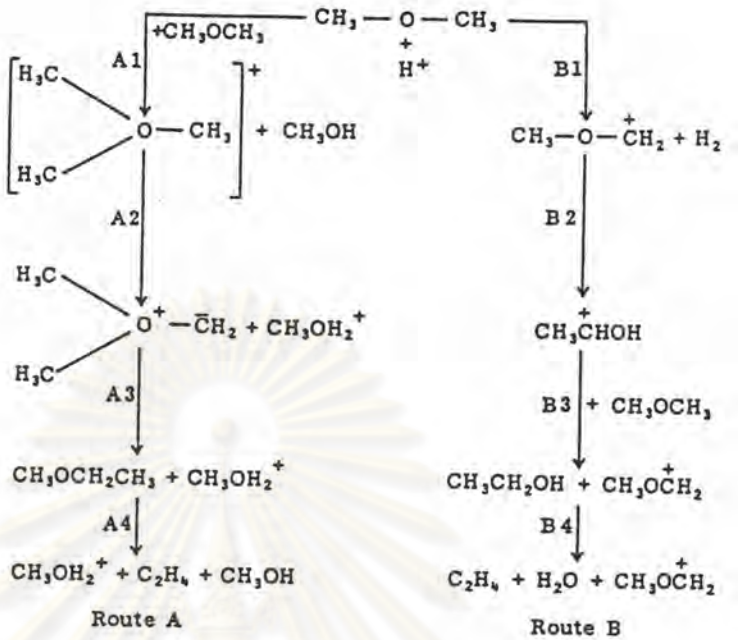

A major difference is found between Steps A2 and B2. However, ab initio calculations indicate that although the 1-hydroxyethyl cation is more stable than the methoxymethyl cation, the energy barrier separating the two is on the order of 260 kJ/mole, assuming that the rearrangement proceeds through the O-protonated oxirane:

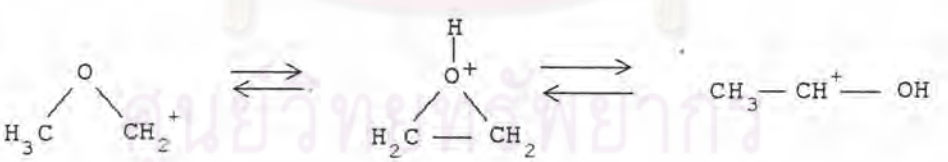

this is comparable to the expected energy barrier of Step A2. Step A3 is highly exothermic and, in viewofthe behavior of the N-analogue, is expected to have a low activation energy. Figure 3.4 is an energy diagram comparing Routes A and B. It was concluded that Route A, involving the trimethyloxonium ion, is favored.

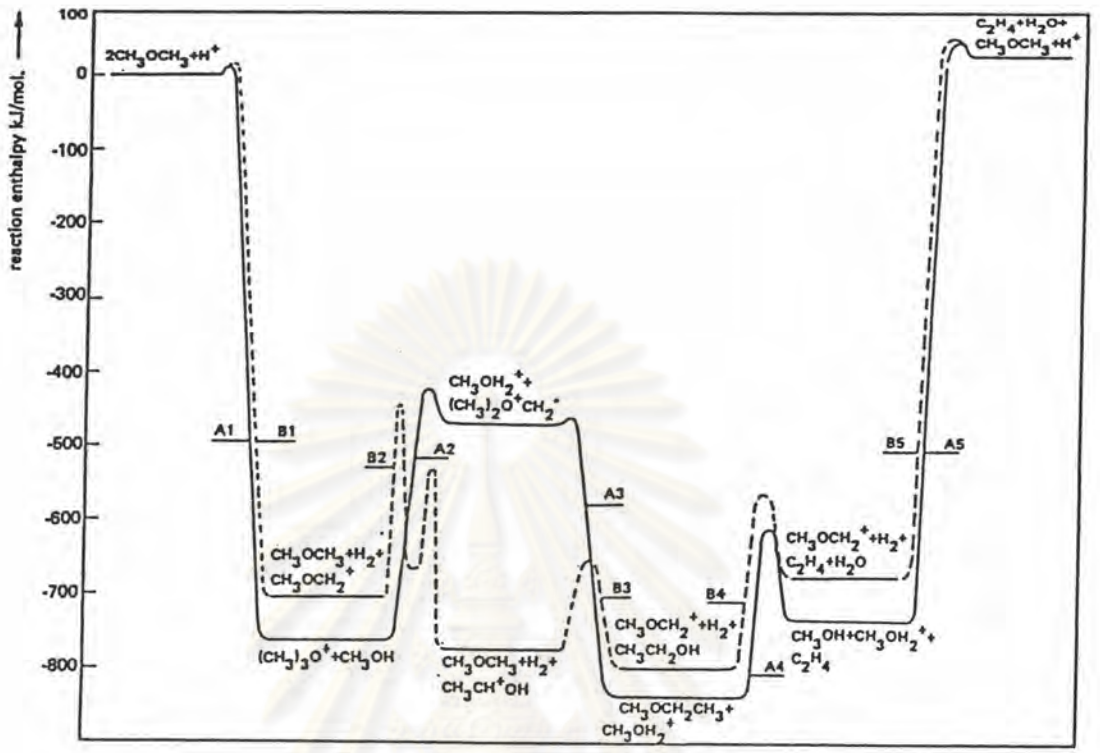

Figure 3.9 Energy diagram for Routes A and B [81].

According to van der Berg, kinetics of dimethyl ether reaction over HZSM-5 is zero-order at 227-300 °C. Chang and Lang found the reaction order of methanol decomposition over HZSM-5 at 371 °C to be zero-order up to about 60% conversion, and increasing in order at higher conversions, suggestive of Langmuir-Hinshelwood behavior. This is consistent with van den Berg's proposal that the formation of adsorbed alkoxyoxonium species is favored, with the C-C bond of formation as the most demanding step. However, van den Berg observed an anomalous temperature effect, illustrated in the Arrhenius plot of Figure 3.10. To explain this phenomenon it was proposed that at 227-260 °C, C-C bond formation proceeds via the intramolecular rearrangement of trimethyloxonium ions while at higher temperatures a

concerted reaction between dimethyl ether and alkyl cations, with the oxonium ion as the transition state, becomes significant.

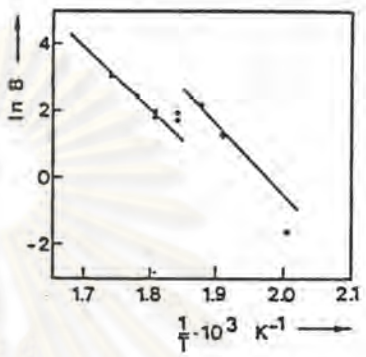

Figure 3.10 Arrhenius plot of the dimethyl ether conversion on zeolite H-ZSM-5 [81]. P_x = 50.7 kPa; WHSV = 0.72 h^{-1}.

It should be noted that ylid mechanisms have been earlier proposed to explain C-C bond formation from organic N and S compounds in the presence of zeolites. One such example is the formation of stilbenefrom benzyl mercaptan over Na13X reported by Venuto and Landis [82]. Although these workers preferred an α-elimination mechanism for this reaction, they recognized that a sulfonium ylid mechanism is also possible. Wu et al. [83] studied the thermal decomposition of methylammonium cation exchanged Y-type faujasites. At 275-450 °C, ethene was observed among the products of decomposition. To account for this result, a mechanism involving a Stevens rearrangement followed by Hofmann elimination was proposed

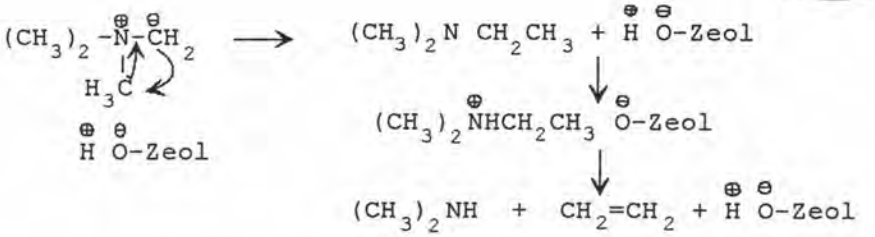

In another example (not involving zeolites) reported by Lepley and Giumanini [84], the thermolysis of N,N-dimethylpyrrolidinium bromide gives N-ethylpyrrolidine by carbene insertion:

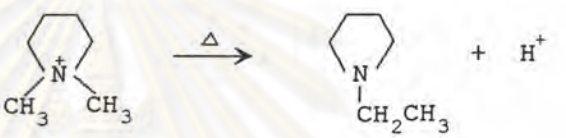

The Stevens rearrangement of oxonium compounds has not been reported up to this time. However, the insertion of CH_2, generated by ketene photolysis, into C-H bonds of alkyl ethers is believed to occur via an ylid intermediate. No insertion into alkyl ether is observed when the methylene is generated by mercury photosensitization, indicating that singlet methylene is involved in the attack. Methylene generated from diazomethane by cuprous halide-catalyzed decomposition was similarly ineffectual. However, when the substrate contains an electron-withdrawing group, reaction with diazomethane occurs, as in the following reaction reported by Meerwein et al. [85]:

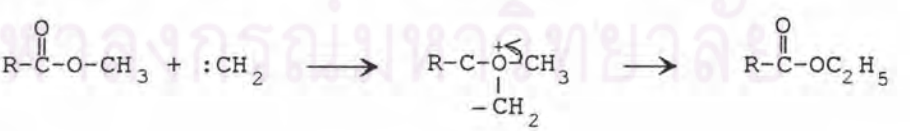

Methanol conversion over phosphorus-modified ZSM-5 was studied by Kaeding and Butter, who proposed the following mechanism based also on oxonium intermediates:

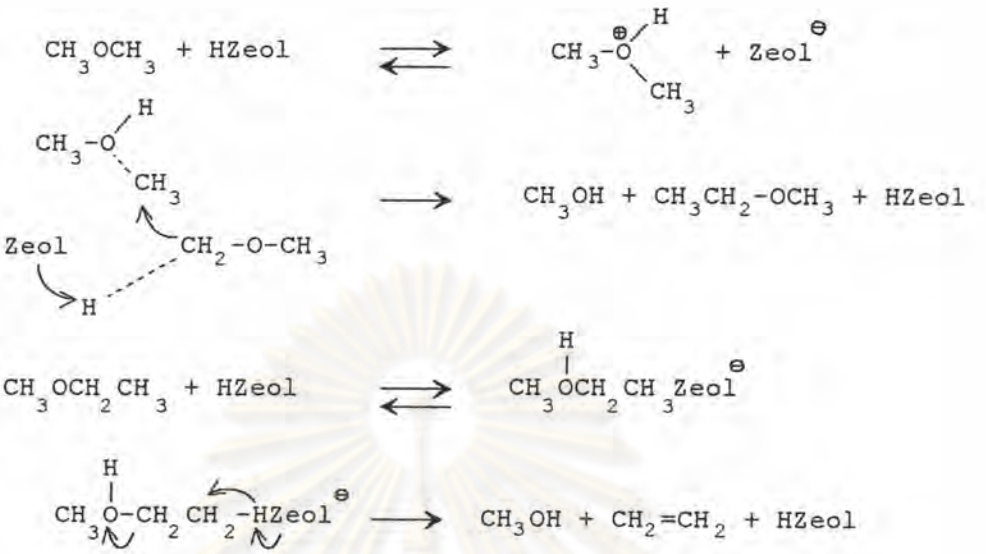

The key step in this mechanism is the labilization of a C-H bond, assisted by anionic sites in the zeolite. The resultant nucleophilic species then attacks the "incipient methyl carbonium ion" from protonated methyl ether (or methanol).

2.4. Carbenium Ions and Superacid Chemistry

Mechanisms based on electrophilic attack by methyl cations at saturated carbon are favored by some workers. Such reactions were first observed insuperacid media by Olah and co-workers and are exemplified by the remarkable reaction of methane:

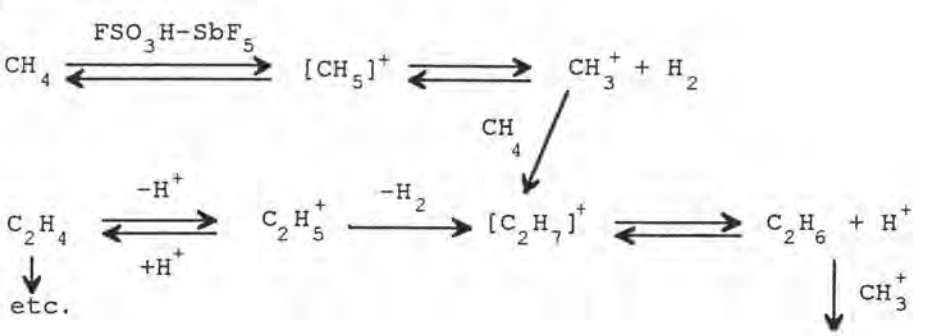

The transition state is believed to be a pentacoordinate carbonium ion, typified by the CH_5^+ methanonium ion shown above, and in the following substitution reaction:

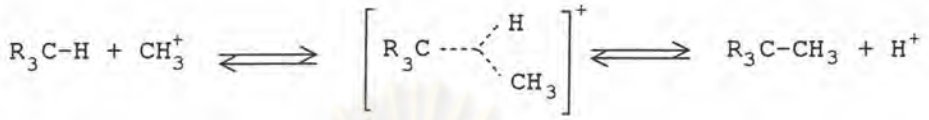

Pearson [86] proposed this as a possible mechanism of C-C bond formation in methanol decomposition by phosphorus pentoxide.

Based on their observation that methanol converts to hydrocarbons over heteropolyacids and Nafion-H (perfluorinated sulfonic acid resin), which are Bronsted acids, Ono and Mori [87] concluded that the mechanism involves methyl cations:

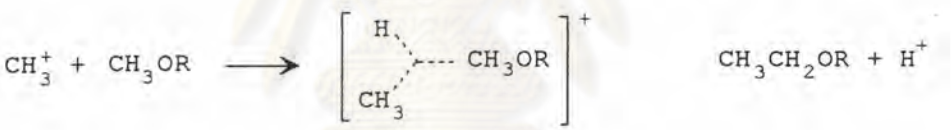

Generation of the methyl cation was considered to occur by polarization of surface methoxyl species:

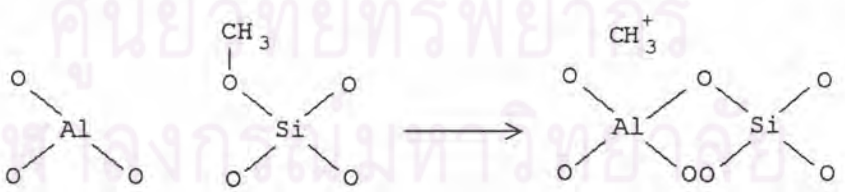

Autocatalysis involving condensation of methanol and olefins was cited as the reason why little methane is produced via hydride abstraction.

Ono et al. rejected the possibility of carbene involvement. They found that HCl did not poison the methanol reaction over HZSM-5. They reasoned that since HCl poisons base-catalyzed reactions, basic sites do not

participate in the reaction. They assert that these results "plead against the carbene mechanism, in which the abstraction of a proton from a methyl group by basic sites is essential."

The Olah superacid mechanism was also favored by Kagi [88], who proposed a series of oxonium intermediates, e.g.,

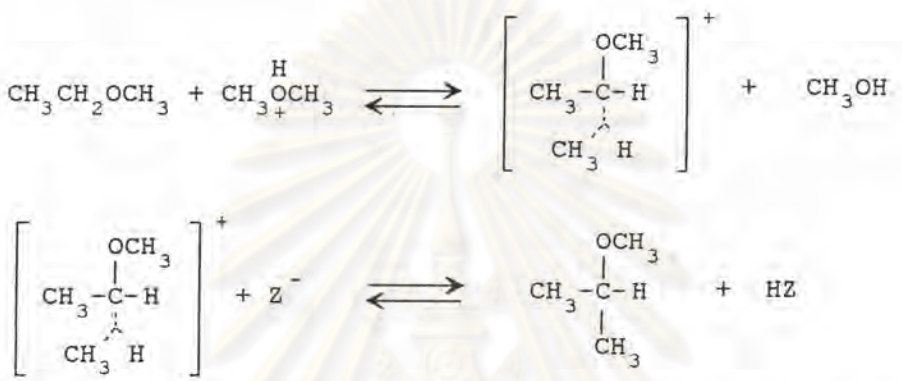

However, Chang considered the bulky transition states arising from such reactions improbable in ZSM-5 on account of limitations due to channel size.

It should be noted that neither CH_3^+ nor CH_5^+ have thus far been directly observed in superacid solutions. It has also been pointed out that SbF_5 and SO_3 are strong oxidizing species and could generate carbenium ions from alkanes by oxidation, although Olah points out that similar carbocation transformations are observed in systems such as HF-TaF_5 and HF-BF_3 which have high redox potentials, and therefore would not be potent oxidizing media.

Salem [89] has reported the conversion of methanol and dimethyl ether to hydrocarbons over TaF_5 and NbF_5. At 300°C in an autoclave, a twofold excess of methanol was converted to a mixture of paraffins and aromatics. The NbF_5-catalyzed reaction gave more light hydrocarbons (>81% C_1-C_5) than the TaF_5 reaction (53% C_1-C_5). It was not clear whether the TaF_5 and NbF_5 were stable to hydrolysis under the reaction conditions or deactivated during the course of reaction.

The conversion of methanol over the alkylammonium zeolite Nu-1 was investigated by Spencer and Whittam [90]. They concluded that strong acidity is needed for the fast initial step and that cationic intermediates are involved. However, neither CH_3^+ nor oxonium ions were considered to be plausible.

2.5. Chain Mechanisms

Anderson et al., using deuterium labeling, found that in the methylation of benzene with methanol over HZSM-5 at 207°C, there is no exchange involving methyl hydrogens. From this it was inferred that in the methanol-to-hydrocarbon reaction, the initial step does not involve lability of the C-H bond prior to C-C bond formation, and that therefore the reactive intermediates are not carbene, carbenoid, or oxymethylene species. Instead, a active C_1 entity of the type $(CH_3)RO^+H$ (R = H or CH_3) was proposed, which participates in a chain propagation mechanism

$$\text{active } C_1 + \text{reactive } C_n \text{ -----> reactive } C_{n+1}$$

where C_n is an olefin. This is a highly attractive scheme in that it is consistent with the observed autocatalysis of the reaction. Insuch a scheme, moreover, the precise nature of the C_1 species becomes somewhat of a moot question. However, as has been noted, the temperature at which these D-labeling experiments were carried out was below the threshold for hydrocarbon formation from methanol in the presence of ZSM-5. Thus their bearing on the mechanistic question may be somewhat tenuous. The results of Matsushima and White[91] on deuterium exchange between CH_3OH and CD_3OD over alumina have already been mentioned. It will be recalled that these authors found little D-exchange below 237°C but complete scrambling at higher temperature ($T \geq 397$°C).